

Dynamics and Nanolevel Structure in an Ionomer Blend of Two Polymers with Widely Separated Glass Transitions

P. Bergquist, J.-F. Shi, J. Zhao, A. A. Jones, and P. T. Inglefield*

Carlson School of Chemistry, Clark University, Worcester, Massachusetts 01610

R. P. Kambour

Materials Laboratory, General Electric Corporate Research and Development, Schenectady, New York 12301

Received October 17, 1996; Revised Manuscript Received November 21, 1997

ABSTRACT: A new ionomer blend of zinc-neutralized sulfonated poly(2,6-dimethyl-1,4-phenylene oxide) and an amino silicone copolymer was prepared. The blend precipitates as a gel from dilute solution and forms a coherent film. Magic angle spinning carbon-13 spectra indicated coordination of the amine of the amino silicone copolymer by the zinc ion. Differential scanning calorimetry and dynamic mechanical spectra show a smearing out of the glass transition over the more than 300 deg temperature separation of the glass transitions of the component polymers. Solid-state proton NMR line shapes indicate narrowing commences at -115°C , but then the line remains a composite of a narrow Lorentzian line and a broad Gaussian line for at least the next 200 deg, in agreement with the dynamic mechanical data. Goldman–Shen proton spin diffusion measurements give a domain size of the order of 30 Å, corresponding to the more mobile protons contributing to the Lorentzian line shape component. Silicon-29 chemical shift anisotropy line shapes demonstrate the onset of mobility for some of the siloxane units beginning at -115°C , but complete line shape collapse does not occur even after a 200 deg temperature rise. This again indicates an extended glass transition process even when considering just one component of the blend.

Introduction

Recent solid-state NMR experiments have revealed details of the repeat unit level dynamics at the glass transition in amorphous polymers and have indicated the inter-relationship of local structural heterogeneities and local dynamic heterogeneities.^{1–4} The local structure and dynamics of a polymeric glass can be modified by blending two polymers or by the introduction of a low molecular weight diluent.^{5–11}

In a compatible polymer blend where the polymeric constituents have T_g 's differing by 100 deg,⁵ the local dynamics associated with the glass transition can nearly collapse to as narrow a temperature range as is observed in a pure amorphous polymer. However inter-related residual dynamic and structural heterogeneities remain and the heterogeneities are controlled by the relative concentration of the constituents. The heterogeneities have dimensions comparable to the size of the repeat units (nanometers) and have been attributed to nearly random concentration fluctuations.^{5,7}

In polymer diluent systems such as polycarbonate plus phosphate esters at diluent concentrations of 5–20 wt %, the reorientational dynamics of the diluent becomes bimodal with an effective separation in temperature of as much as 200 deg between the dynamics of the diluent surrounded by polymer and diluent molecules in contact with other diluent molecules.^{8–11} If reorientational freedom is associated with the glass transition, then part of the diluent undergoes the transition at one temperature and the remainder at another. The glass transition of the pure diluent (a phosphate ester) is about 300 deg less than that of the polymer. Again, it is nanolevel heterogeneities produced by random concentration fluctuations that are associated with the bimodal dynamics.

The motivation that led to the study of the ionomer blend presented here was to produce a polymer blend from two constituent polymers having glass transition temperatures separated by 300 deg. In such a case, what would be the nature of the local dynamics and the local structure associated with reorientational freedom and the glass transition? Could the blending be controlled to produce different dynamics and associated nanostructures?

The problem in making a blend of two polymers with such widely separated glass transition ranges is that such systems involve fundamentally incompatible polymers if one considers such standard measures as solubility parameters. To overcome the incompatibility, an ionomer form and an amine-containing copolymer form, respectively, of two polymers with widely separated T_g 's are used in conjunction with coordination chemistry to achieve a chemically based interaction to drive the system toward compatibility.^{12–17} The high T_g polymer selected is zinc-neutralized sulfonated poly(2,6-dimethyl-1,4-phenylene oxide) and the low T_g polymer is a copolymer of dimethylsiloxane and methyl-(aminopropyl)siloxane. The glass transition separation of the starting polymeric materials is over 300 deg.

Experimental Section

An amino silicone copolymer (a-silicone) from Genesee Polymers Corp. with 6.45 mol % aminopropyl groups in place of one of the methyl groups on the backbone silicon is used as one component of the blend (mol wt 4892). A zinc-neutralized sulfonated poly(2,6-dimethyl-1,4-phenylene oxide) ionomer (ZnSPXE) was used as the other component of the blend. The sulfonation level (on the meta position of the ring) is 10 mol %. The ZnSPXE and the a-silicone were dissolved in dry dimethyl sulfoxide and tetrahydrofuran, respectively, at the level of a few weight percent. The relative stoichiometry was

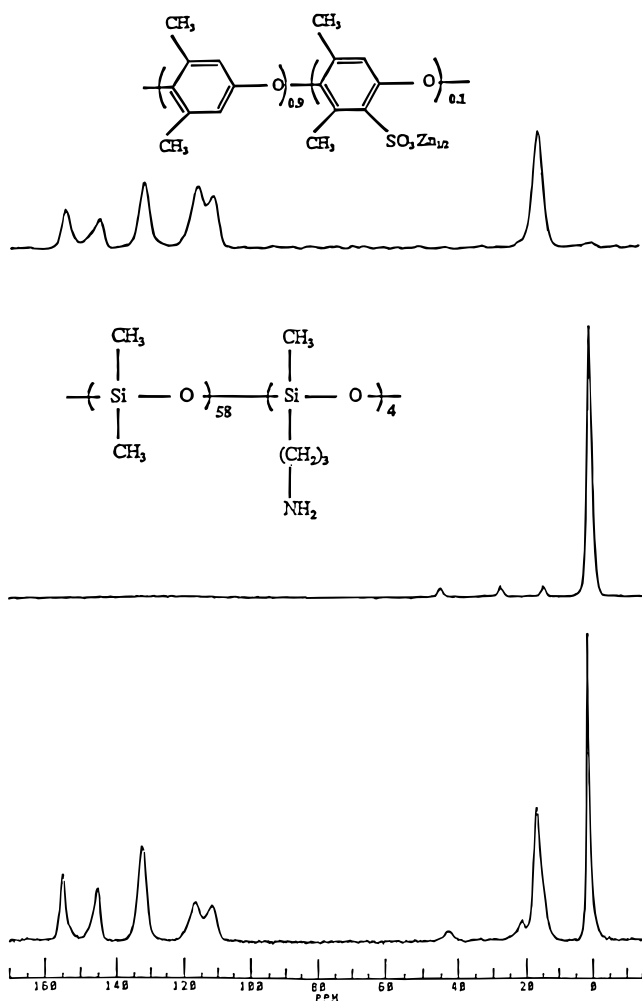


Figure 1. Structures and carbon-13 magic angle spinning spectra of the starting materials and the blend. The peak at 45.0 ppm of the amino silicone is the terminal carbon of the propylamine group, and it shifts to 42.3 ppm in the blend after coordination of the zinc ion by the amine nitrogen.

set at one zinc ion per amine. A second synthesis was also carried out in which an excess of the amine was employed, the Zn ion-to-amine ratio being 1:1.33 (the resultant blend compositions are estimated from the relative methyl intensities corresponding to the two components in the ^{13}C NMR spectrum). The two homogeneous solutions were mixed, at which point the mixture became turbid. After a period of days, a gel was formed which precipitated out of solution. The supernatant liquid was then poured off, leaving the gel as a coherent film that was washed with dry acetone and vacuum-dried for several days.

Dynamic mechanical spectra of the blend were taken on a Seiko DMS210 Tensile Module at frequencies of 1, 5, and 20 Hz, and differential scanning calorimetry on a Perkin-Elmer 7 Series/UNIX DSC 7 was applied to the starting materials as well as the blend.

All NMR experiments were performed on a Bruker MSL 300, including magic angle carbon-13 spectra, proton wide line spectra, proton Goldman-Shen¹⁸ domain size experiments, and silicon-29 chemical shift anisotropy line shape experiments.

Results and Interpretation

Carbon-13 magic angle spinning spectra of the two starting materials and the polymer blend are shown in Figure 1 along with the structures of the starting materials. Note that the extent of reaction can be monitored by the resonance at 45.0 ppm from the amino

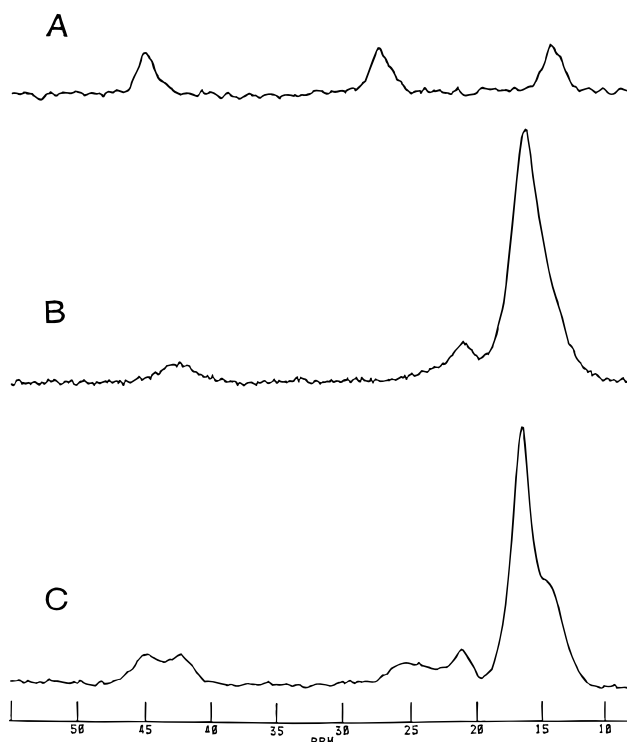


Figure 2. Expanded carbon-13 magic angle spinning spectra. The starting material, amino silicone (A), is compared to a blend formed at a 1 to 1 stoichiometry (B) and a blend prepared in an excess of amino silicone (C). The presence of a carbon resonance at 45.0 ppm as well as 42.3 ppm in the excess amino silicone blend indicates both reacted and unreacted amine groups in this blend, while the absence of a signal at 45.0 ppm in the 1 to 1 blend indicates nearly complete reaction of the amine groups in this case.

silicone, which corresponds to the terminal carbon of the propyl group bearing the amine. In the blend this resonance is absent and a new line appears at 42.3 ppm, which is interpreted as indicating nearly complete coordination of the amine by the zinc ion. The blend spectrum shown in Figure 1 was prepared from a starting stoichiometry of 1 zinc ion per 1 amine group. In Figure 2, the region around 40 ppm is expanded and the starting material is compared to the blend prepared from a 1 to 1 stoichiometry, as just discussed, as well as a blend prepared from a solution containing an excess of amino silicone. In the blend with excess amino silicone, a resonance corresponding to uncoordinated amine at 45.0 ppm is present as well as the resonance indicating coordinated amine at 42.3 ppm. This indicates that the blend can be prepared with different ratios of the two starting materials and the level of cross-linking produced by coordination of the zinc ion can be controlled and monitored. Thus the magic angle spectra provide direct evidence of the reaction producing this ionomer blend and a convenient monitor of the extent of the reaction.

In Figure 3, DSC results are given for the amino silicone and ZnSPXE starting materials and the 1 to 1 blend. A glass transition at -116°C is observed in the amino silicone, and there is no indication of any melting of crystallites. Apparently, no crystallization is present in the amino silicone copolymer. In the blend, almost no transition can be seen, though a weak, broad response starting at about the same temperature may be present. In the high-temperature region a transition for the ZnSPXE starting material is seen at 240°C ,

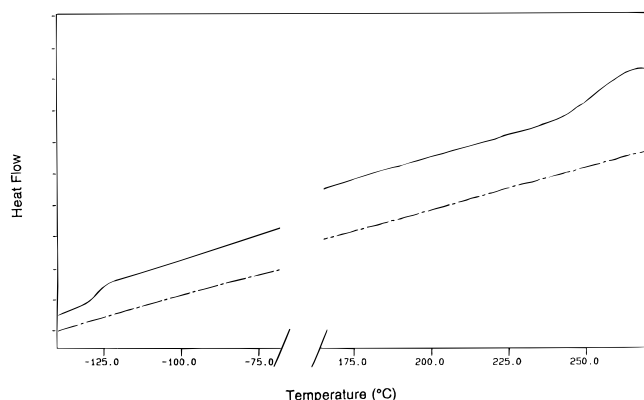


Figure 3. DSC thermograms. (Left) The amino silicone starting material (—) shows a standard glass transition near $-116\text{ }^{\circ}\text{C}$, and the 1 to 1 blend (---) shows almost no indication of a transition in the same region. (Right) The ZnSPXE starting material (—) shows a glass transition near $240\text{ }^{\circ}\text{C}$, and the 1 to 1 blend (---) shows almost no evidence of a transition in the same region.

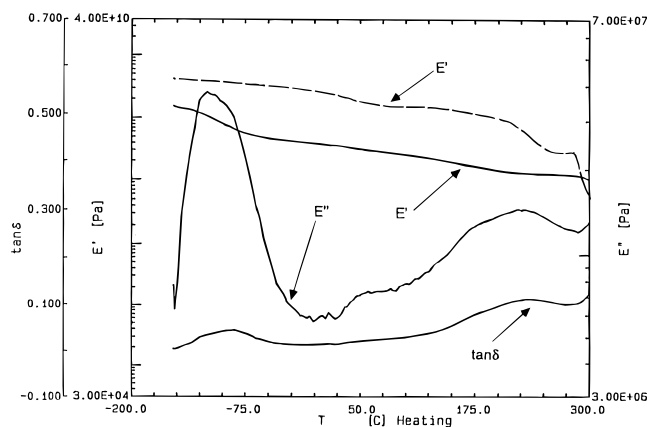


Figure 4. Dynamic mechanical response of the ZnSPXE starting material (---) and the 1 to 1 blend (—) at 20 Hz as a function of temperature. E' and E'' represent the storage and loss modulus, respectively, and the different ordinate axes serve to identify the magnitudes of the different responses.

which is near the glass transition temperature of poly(phenylene oxide) without sulfonate groups and again the 1 to 1 blend shows a greatly diminished response at about $190\text{ }^{\circ}\text{C}$. Essentially, standard differential scanning calorimetry is not able to clearly identify the transitions in this system but does show the absence of large changes in the thermal properties at the temperatures of transitions in the starting materials.

Dynamic mechanical spectra of the ZnSPXE starting material and the 1 to 1 blend are shown in Figure 4. No mechanical spectra could be obtained on the amino silicone since it became a viscous fluid just above the DSC transition temperature. The modulus (E') of the ZnSPXE starts dropping at about $200\text{ }^{\circ}\text{C}$, indicating the same glass transition range as the DSC results. For the 1 to 1 blend, the modulus starts dropping at about $-120\text{ }^{\circ}\text{C}$ and continues to drop continuously for the next 370 deg . There is no sharp drop in the modulus of the blend starting at $200\text{ }^{\circ}\text{C}$ as there is in the pure ZnSPXE. There are two more pronounced loss modulus peaks (E'') in the blend at -110 and $+225\text{ }^{\circ}\text{C}$ in the general region of the transition ranges of the starting materials, but these loss peaks are of low amplitude, with E'' being a factor of 40 lower than E' for the lower temperature peak. The relatively low magnitude of the relaxation processes are also indicated by $\tan \delta$, which is about

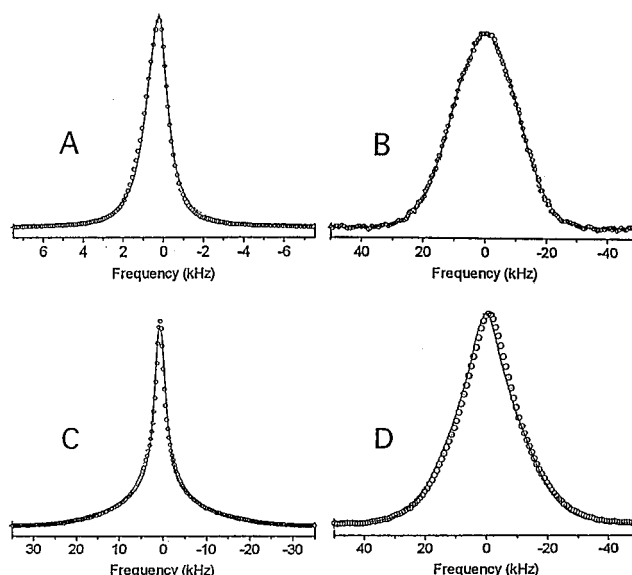


Figure 5. Proton line shapes at a temperature of $-93\text{ }^{\circ}\text{C}$: (A) amino silicone starting material; (B) ZnSPXE starting material; (C) excess amino silicone blend; (D) 1 to 1 blend. At this temperature, the ZnSPXE is a broad Gaussian, the pure amino silicone is a narrow Lorentzian, and the blends are a composite of both types of line shapes. The lines represent fits to the experimental points based on these line shapes.

0.06 for the lower temperature relaxation. There is also loss observed at all temperatures between these two peaks, indicative of a smearing out of the relaxations corresponding to the α transitions of the starting materials. The implications of this will be discussed further.

Representative proton line shapes at low temperature for the starting materials and the blends are presented in Figure 5. The amino silicone displays typical proton line narrowing for an amorphous glass with a transition temperature around $-115\text{ }^{\circ}\text{C}$. Below that temperature, the line is a broad Gaussian and above that temperature it becomes a narrow Lorentzian. Figure 6a is a plot of line width versus temperature. The ZnSPXE line shape remains a broad Gaussian over the accessible temperature range (up to $100\text{ }^{\circ}\text{C}$), and its line width is also given as a function of temperature in Figure 6a. The 1 to 1 blend line shape begins narrowing at $-115\text{ }^{\circ}\text{C}$, but thereafter the line shape is neither a Gaussian nor a Lorentzian. It can, however, be fit as a sum of a broad Gaussian and a narrow Lorentzian with the fractional population of Gaussian component decreasing with temperature. The line widths of the Gaussian and Lorentzian components are plotted in Figure 6a as a function of temperature and the fractional population of Gaussian component is plotted in Figure 6b. Also shown in Figure 6 are the proton line width results for the blend prepared with an excess of amino silicone corresponding to the carbon-13 MAS spectrum shown in Figures 1 and 2. Qualitatively, both blends are similar but the lines narrow more rapidly with temperature in the blend containing unreacted amine groups. In both cases the mobility in the blends shows significant changes relative to the parent species: in the 1:1 blend the mobile component is considerably restricted dynamically relative to pure amino silicone, as indicated by a line width that is larger by a factor of 10 above $-100\text{ }^{\circ}\text{C}$. In the blend containing excess amino silicone it is the rigid component that exhibits a significant departure from the behavior of the parent ZnSPXE with

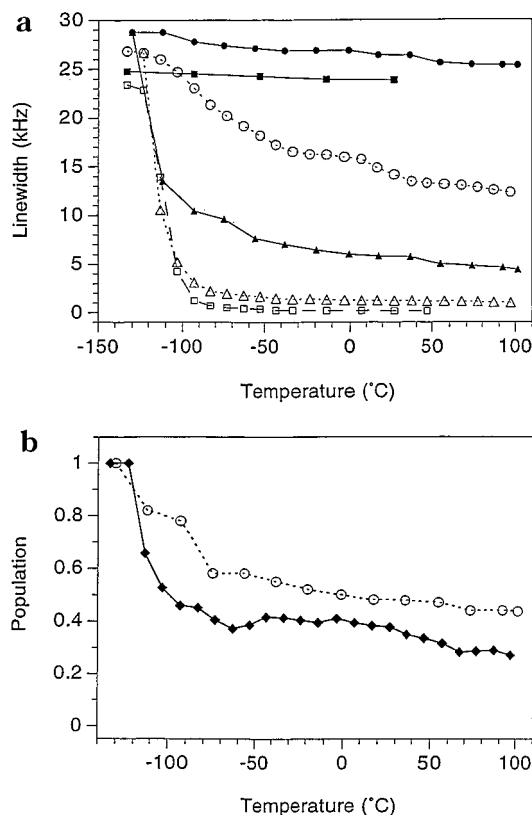


Figure 6. (a) Proton line widths versus temperature: (a) amino silicone starting material (\square); (b) ZnSPXE starting material (\blacksquare); (c) 1 to 1 blend: rigid component (\bullet) and mobile component (\blacktriangle); (d) excess amino silicone blend: rigid component (\circ) and mobile component (\triangle). (b) Fraction of proton line shape that is a broad gaussian: (a) one to one blend (\circ); (b) excess amino silicone blend (\blacklozenge).

a line width that is a factor of 2 narrower above -100 °C. These observations imply a dynamic heterogeneity in these materials intermediate between a compatible blend such as PXE/polystyrene⁵ and a dynamically decoupled situation such as exists in a classical SBS block polymer.

In bimodal line shapes of the type seen in this blend, proton spin diffusion measurements can be performed to determine the size of the domain corresponding to the narrow or Lorentzian component. Such experiments have been performed to determine domain sizes in semicrystalline polymers^{19,20} and polymer-diluent mixed glasses.¹¹ In the simple Goldman-Shen¹⁸ (GS) experiment, discrimination times of 80–100 μ s were found to separate the narrow component from the broad component. Free induction decays (FID's) taken with different mix times after the discrimination period ranging from 4 to 500 ms. At short mix times, an exponential decay corresponding to the Lorentzian component is observed. As the mix time is increased, a rapidly decaying component corresponding to the broad Gaussian shape reappears, indicating spin diffusion from the more mobile, narrow component to the less mobile broad component.

Each FID in the GS experiment can be fit to an equation^{19,20} of the form

$$G(t) = Ae^{-(t/T_{21})^2} + (1 - A)e^{-(t/T_{2m})} \quad (1)$$

The spin-spin relaxation time of the less mobile component in the GS experiment is T_{21} and a Gaussian form

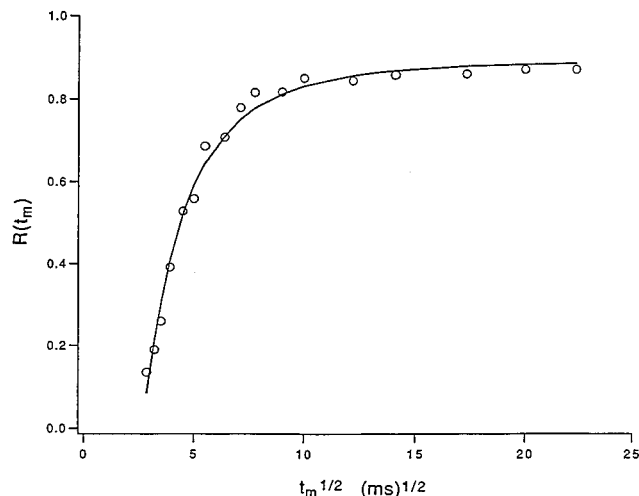


Figure 7. Goldman-Shen spin diffusion recovery curve for the 1 to 1 Blend at 300 K. The line is a fit based on 3D diffusion and allows for variation of the long-time limit.

Table 1

temp (K)	t_0 (μ s)	D/b^2 (ms^{-1})	b (\AA)	D ($10^{-12} \text{ cm}^2 \text{ s}^{-1}$)	T_{2m} (μ s)	T_{21} (μ s)
1 to 1 Blend						
319	80	0.0107	31.0	1.03	73	18.4
Excess Amino Silicone Blend						
300	100	0.0095	33.0	1.03	320	41.0

for the time dependence is assumed. The spin-spin relaxation of the more mobile component in the GS experiment is T_{2m} , and a time dependence corresponding to a Lorentzian is assumed. The quantity A is a function of mix time and is used to monitor the repopulation of the broad Gaussian component following the selection of the narrow component in the first part of the GS experiment. The recovery of the less mobile component in the GS experiment is monitored by the quantity $R(t_{\text{mix}})$ where

$$R(t_{\text{mix}}) = A(t_{\text{mix}})/A(\infty) \quad (2)$$

where $A(\infty)$ is the population of the less mobile Gaussian component at time infinity in the absence of any spin-lattice relaxation. The proton spin-lattice relaxation time in the blend is approximately 1 s.

Expressions for the recovery factor as a function of mix time based on spin diffusion have been developed by Cheung and Gerstein.²¹ The key parameters are the spin diffusion constant, D , and the domain size b . The Cheung and Gerstein expression neglects spin-lattice relaxation and assumes a random distribution of more mobile domains in the sample. The three-dimensional form of the recovery equation suited for the sample under consideration is

$$R(t) = 1 - \phi_x(t) \phi_y(t) \phi_z(t) \quad (3)$$

where each $\phi(t)$ has the form

$$\phi(t) = \exp(Dt/b^2) \text{erfc}(Dt/b^2)^{1/2} \quad (4)$$

Figure 7 shows a typical recovery curve fit to eqs 3 and 4. For a series of temperatures, mix times and blend compositions, Table 1 lists the values of D/b^2 obtained from eq 3 in the fitting process.

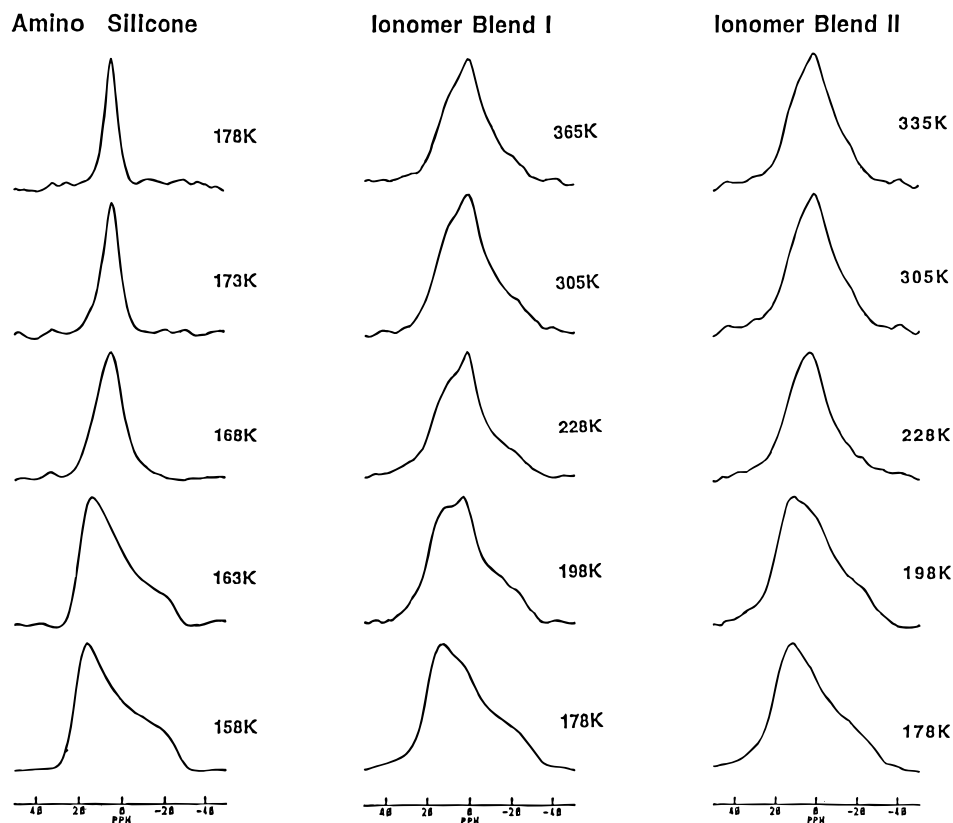


Figure 8. Silicon-29 chemical shift anisotropy line shapes versus temperature.

To obtain a value for b as a measure of domain size, D will be estimated from the equation presented by Cheung and Gerstein.²¹

$$D = 0.13a^2/T_{21} \quad (5)$$

where a is the average distance between adjacent protons in the less mobile domain. It should be noted that the value for D , determined by static dipolar couplings, is undoubtedly different in the two domains and at differing mix times relative to the value of b^2/D , this should be explicitly included in the analysis. This has been discussed in detail previously,^{21,22} and the assumption of equal spin diffusion constants in both domains assumed in the derivation of eq 4 does not alter the general magnitude of the domain size determination. In this case there is likely a distribution of sizes present and the determination here serves to indicate the average size. Somewhat arbitrarily, a is set at 1.8 Å, corresponding to the intramolecular separation of methyl and aromatic protons. Given this choice for D , values of D and b are tabulated in Table 1 along with T_{2m} and T_{21} .

Silicon-29 chemical shift anisotropy (CSA) line shapes can be obtained to compare glass transition dynamics in the pure amino silicone with the dynamics of this component in two blends (one with excess amino silicone and one with the 1 to 1 composition). Figure 8 shows the line shapes for the three types of materials obtained immediately after cross polarization. The proton spin reservoir in this case is dominated by methyl groups, which undergo rapid rotation over the entire temperature range. Experimentally, it is observed that the partially collapsed silicon-29 line shapes do not depend on the length of the cross-polarization time in the range of 1–8 ms. It appears that the effectiveness of cross

polarization is not strongly influenced by the presence or absence of the segmental motion of the siloxane backbone, which is much slower than methyl group rotation. Cross polarization is occurring from a proton line that is always at least partially narrowed, and the only experimental problem was the relative sharpness of the Hartman–Hahn match.

The silicon-29 CSA line shapes of the pure amino silicone appear much like carbon-13 CSA line shapes near the glass transition, so an interpretation similar to that developed for other amorphous polymers seems plausible. The silicon-29 line shape collapse of the pure amino silicone starts near the transition temperature observed by DSC. In the other polymers, the backbone units undergo Brownian rotational diffusion with an apparent distribution of correlation times^{1,5–6} and the distribution of correlation times commonly covers 3 orders of magnitude, which leads to line shape collapse over a range of about 15 deg. In contrast, the silicon-29 CSA line shapes on the blend begin collapse at the same temperature as the pure amino silicone but only a fraction of the nuclei contributing to the line shape undergo collapse in that temperature region. The majority of silicon nuclei are not reorienting either rapidly or isotropically at the highest temperature studied, 200 deg above the temperature at which collapse begins.

Discussion

The reaction that produces the blend by precipitation of a gel from dilute solution can be considered from the standpoint of the formation of an infinite network where the amino silicone is viewed as a tetrafunctional cross-linking agent. There are, on average, four propylamine functionalities on each amino silicone chain, and to achieve an infinite network, the probability α that one

amino silicone chain is connected through the coordinating ion has to exceed the critical value,²³ $\alpha_c = 1/(f - 1)$ where $f = 4$, the functionality of the amino silicone chains. In the 1 to 1 blend the carbon-13 MAS spectrum shows α to be 1, while in the excess amino silicone blend α is $1/2$. In both cases the value of α_c is exceeded, indicating the formation of an infinite network. No blend has been prepared as yet with an α as small as $1/3$, though this is at least theoretically possible.

The original purpose of preparing this blend was to study the dynamics associated with the glass transition process. DSC gives only a rather weak, broad indication of transitions, while dynamic mechanical spectroscopy gives a more dramatic indication of the smearing out of the glass transition process over the 300 deg separation between the transition temperatures of the starting materials. There is a fairly continuous monotonic drop in modulus starting at about -115°C and extending above 220°C . There are small loss peaks at the transition temperatures of the polymeric components (-115 and $+220^\circ\text{C}$), but there is substantial loss at intermediate temperatures as well. The origin of the monotonic drop in modulus is thought to arise from some dynamic coupling between the more mobile and less mobile regions. The length scale of the heterogeneities in this system are of the order of tens of Angstroms. This places the morphology between a very compatible blend system such as PXE/PS where the length scale is below 10 \AA and a system exhibiting well-defined phase separation behavior such as an SBS block copolymer. In block copolymer systems, the glass transition of each component is quite sharp so that in the SBS case²⁴ the width of the transition of the modulus with temperature is about 10 deg for the lower temperature process while the width of the modulus changes observed in the blend studied here is spread over several tens of degrees. In fact, as mentioned above, the sharp drop in modulus of the starting material ZnSPXE is not present in the blend, as shown in Figure 3.

The NMR line shape studies reinforce the dynamic mechanical data. Proton line shapes for the blend show both a broad component and a narrow component. The narrow component is roughly attributed to the more mobile amino silicone chains and the broad component to the more rigid ZnSPXE chains. In the 1 to 1 blend, the rigid component is broader than in the ZnSPXE starting material, indicating the cross-linking process has further restricted motion of the more rigid component. However, in the excess blend the broader component drops fairly rapidly after the glass transition range of amino silicone, indicating significant plasticization of the ZnSPXE component. Of course, the narrower component of the blend is broader than the amino silicone starting material, especially in the 1 to 1 blend, indicating the expected effects of cross-linking to a more rigid component.

Since the proton line shape was distinctly bimodal, it is straightforward to seek the spatial size of the more mobile component by proton spin diffusion experiments. The 1 to 1 blend had mobile domains of about 30 \AA , indicating the nanoscale of the dynamic heterogeneities of this blend. As the level of cross-linking was reduced in the excess amino silicone blend, the heterogeneities became slightly larger (similarly determined by proton spin diffusion measurements). Thus changing the extent of coordination cross-links changes both the

segmental mobility of the blend (as evidenced by the T_g 's) and the associated morphological structure. The small magnitude of the domain size increase estimated in the silicone rich blend reflects the cube root of the volume increase in silicone content (ca. 30%) to a first approximation. The size of these heterogeneities is larger than is observed in the compatible blend of polystyrene and PXE⁷ or in the mixed glasses produced by adding diluents to amorphous polymers.¹¹ They are also smaller than is observed in a phase-separated block copolymer if the block lengths are long.

Silicon-29 CSA line shapes provided information specifically on the mobility of the silicon amine component of the blend. For comparison, as a pure material the amino silicone undergoes a glass transition at about -115°C , which produces complete line shape collapse in 15 or 20 deg . In the blend, collapse begins at the same temperature but complete collapse is not achieved for hundreds of degrees. This is very direct evidence of the smearing out of the glass transition process associated with the segmental mobility of the amino silicone chains. In fact, given such a wide temperature range required to achieve segmental mobility it becomes unclear how to define a glass transition temperature for this blend. The modification of the transition process by adjustment of the extent of coordination cross-links is also clear in the silicon-29 CSA spectra as it was in the proton spectra. More mobility is produced when the unreacted propylamine groups are present in the blend. However, since the silicon-29 CSA spectra show the presence of relatively immobile siloxane units as well, the domain size determined from proton Goldman-Shen experiments most likely reflects a mobile region consisting of only a fraction of the siloxane repeat units. The rigid siloxane units are probably close to the aminopropyl groups and thus closer to the coordination cross-links to the more rigid phenylene oxide units. The more mobile siloxane units must be more distant from cross-link sites and possibly include portions of siloxane chain between several different cross-link points.

Conclusion

The goal of preparing a blend of two polymers with widely differing glass transition temperatures was achieved. The blend has larger structural heterogeneities associated with dynamic domains than the other well-studied compatible blend (PXE/PS). Also the glass transition of this new blend does not collapse to a relatively narrow, intermediate temperature but is spread out over about 200 deg with the mobility of each component influenced by the other with the extent of the influence controlled by the number of unreacted propylamine groups. Relative to mixed glasses of a polymer and a diluent in which the glass transition temperature of the starting materials also differed by 300 deg , the ionomer blend shows more of a smearing out of reorientational motion associated with the glass transition process while the polymer-diluent system showed a more distinctly bimodal behavior. Either the cross-links in the ionomer blend or the nature of segmental motion in a polymer leads to a stronger coupling of motion between the two components than was observed for the polymer-diluent systems. Possibly, both factors contribute to the dynamic coupling of the two different chains in this blend. The mobile regions are not simply associated with all the siloxane components, as shown by the silicon-29 CSA spectra,

since there are also relatively immobile siloxane units. Other morphological experiments are being performed and will be reported later to further characterize the domain structure of the two polymers and the ionic groups leading to coordination cross-links.

Acknowledgment. This research was carried out with the financial support of the National Science Foundation Grant DMR9303193. P.B. wishes to acknowledge support from ONR AASERT Grant No. N000149310994.

References and Notes

- (1) Schmidt-Rohr, K.; Spiess, H. W. *Multidimensional Solid-State NMR and Polymers*; Academic Press: New York, 1994.
- (2) Li, K. L.; Jones, A. A.; Inglefield, P. T.; English, A. D. *Macromolecules* **1989**, *22*, 4198.
- (3) Schmidt-Rohr, K.; Spiess, H. *Phys. Rev. Lett.* **1991**, *66*, 3020.
- (4) Heuer, A.; Wilhelm, M.; Zimmermann, H.; Spiess, H. *Phys. Rev. Lett.* **1995**, *75*, 2851.
- (5) Chin, Y. H.; Zhang, C.; Wang, P.; Inglefield, P. T.; Jones, A. A.; Kambour, R. P.; Bendler, J. T.; White, D. M. *Macromolecules* **1992**, *25*, 3031. Chin, Y. H.; Inglefield, P. T.; Jones, A. A. *Macromolecules* **1993**, *26*, 5372.
- (6) Chung, G.-C.; Kornfield, J. A.; Smith S. D. *Macromolecules* **1994**, *27*, 964, 5792.
- (7) VanderHart, D. L. *Macromolecules* **1994**, *27*, 2837.
- (8) Kambour, R. P.; Kelly, J. M.; McKinley, B. J.; Cauley, B. J.; Inglefield, P. T.; Jones, A. A. *Macromolecules* **1988**, *21*, 2937.
- (9) Cauley, B. J.; Cipriani, C.; Ellis, K.; Roy, A. K.; Jones, A. A.; Inglefield, P. T.; McKinley, B. J.; Kambour, R. P. *Macromolecules* **1991**, *24*, 403.
- (10) Liu, Y.; Turnbull, M. M.; Jones, A. A.; Inglefield, P. T.; Kambour, R. P. *Solid State NMR* **1993**, *2*, 289.
- (11) Liu, Y.; Inglefield, P. T.; Jones, A. A.; Kambour, R. P. *Magn. Reson. Chem.* **1994**, *32*, 518.
- (12) Fitzgerald, J. J.; Weiss, R. A. *Macromol. Chem. Phys.* **1988**, *C28* (1), 99.
- (13) Peiffer, D. G.; Duvdevani, I.; Agarwal, P. K.; Lundberg, R. D. *J. Polym. Sci., Polym. Lett.* **1986**, *24*, 581.
- (14) Lundberg, B. R. D.; Phillips, R. R. *J. Polym. Sci., Polym. Phys.* **1989**, *27*, 245.
- (15) Simmons, A.; Eisenberg, A. *Polym. Prepr. (Am. Chem. Soc., Div. Polym. Chem.)* **1986**, *27*, 341.
- (16) Lu, X.; Weiss, R. A. *Macromolecules* **1991**, *24*, 4381.
- (17) Douglas, E. P.; Waddon, A. J.; MacKnight, W. J. *Macromolecules* **1994**, *27*, 4344.
- (18) Goldman, M.; Shen, L. *Phys. Rev.* **1966**, *144*, 321.
- (19) Assink, R. A. *Macromolecules* **1978**, *11*, 1233.
- (20) Assink, R. A. *J. Polym. Sci., Polym. Phys. Ed.* **1977**, *15*, 59.
- (21) Cheung, T. T. P.; Gernstein, B. C. *J. Appl. Phys.* **1981**, *52*, 5517.
- (22) Li, K.-L.; Jones, A. A.; Inglefield, P. T.; English, A. D. *Macromolecules* **1989**, *22*, 4198.
- (23) Flory, P. J. *Principles of Polymer Chemistry*; Cornell University Press: Ithaca, NY, 1953; p 347.
- (24) McCrum, N. G.; Read, B. E.; Williams, G. *Anelastic and Dielectric Effects in Polymeric Solids*; John Wiley & Sons: New York, 1967; p 419.

MA961533O